Article

Not peer-reviewed version

Physiological Evaluation of Salt Tolerance on Different Genotypes of Sunflower Germplasms at the Seedling Stage

Fangyuan Chen , Lvting Xiao , Qixiu Huang , Lijun Xiang , Qiang Li , Xianfei Hou , Zhonghua Lei * , Youling Zeng *

Posted Date: 23 October 2024

doi: 10.20944/preprints202410.1786.v1

Keywords: Salt tolerant and sensitive sunflower germplasms; Seedling stage; Phenotypes and physiological indicators; The evaluation of salt

Article

Physiological Evaluation of Salt Tolerance on Different Genotypes of Sunflower Germplasms at the Seedling Stage

Fangyuan Chen [1,2], Luting Xiao [1], Qixiu Huang [3], Lijun Xiang [3], Qiang Li [3], Xianfei Hou [3], Zhonghua Lei [3,*] and Youling Zeng [1,*]

[1] Xinjiang Key Laboratory of Biological Resources and Genetic Engineering, College of Life Science and Technology, Xinjiang University, Urumqi, 830017, China.
[2] Key Laboratory of microbial resources protection, development and utilization, College of Biological Sciences and Technology, Yili Normal University, Yining, 835000, China.
[3] Institute of Economic Crops, Xinjiang Academy of Agricultural Sciences, Urumqi, 830091, China.
* e-mail: Youling Zeng (zeng_ylxju@126.com); Zhonghua Lei (youkui@sina.cn). Dr Zeng is fully responsible for the distributions of all materials associated with this article.

Abstract: Sunflower (*Helianthus annuus* L.) is an important oilseed crop cultivated extensively across the globe. High salinity adversely impacts plant growth and physiological processes. In this study, the data of the phenotypes and various indices were collected to clarify the physiological mechanisms underlying sunflower's salt tolerance with the seedlings of two salt-tolerant (182265 and 182283) and two salt-sensitive (182093 and 186096) genotypes, which were exposed to 350 mM NaCl for 4 days. The findings revealed that, during the seedling stage, salt-tolerant sunflowers accumulated less Na^+ and more K^+, resulting in a higher K^+/Na^+ ratio that mitigated ionic toxicity throughout the plants, compared to the salt-sensitive resources. Furthermore, the salt-tolerant germplasms also exerted salt tolerance through the following several pathways: they maintained robust osmotic regulation by accumulating higher levels of proline, soluble sugars, and other osmolytes; they neutralized reactive oxygen species (ROS) by elevating the activity of antioxidant enzymes; and they sustained optimal growth by boosting photosynthesis. Taken together, this study provided a more comprehensive assessment of the sunflower's physiological salt tolerance, offering valuable insights for further exploration of the molecular mechanisms of salt tolerance and accelerating the breeding process for sunflower varieties with improved salt resilience.

Keywords: Salt tolerant and sensitive sunflower germplasms; Seedling stage; Phenotypes and physiological indicators; The evaluation of salt tolerance

Introduction

High salinity impedes plant growth and reduces crop yields by disrupting normal physiological and biochemical processes (Zhao et al., 2020). Initially, under high salt conditions, a substantial influx of Na^+ ions into plant cells leads to ion toxicity, which can be detrimental to cellular function (Zhang et al., 2022). Subsequently, the plant's osmotic regulation capacity is compromised, restricting cell expansion and growth, and hindering the uptake of water and nutrients from saline soils (Shabala et al., 2014). Moreover, osmotic stress triggers rapid stomatal closure, which prevents CO_2 from entering plant cells, and thereby disrupting the process of photosynthesis (Zhao et al., 2020; Shumilina et al., 2019). Furthermore, the excessive accumulation of reactive oxygen species (ROS), such as superoxide anion (O_2^-), hydrogen peroxide (H_2O_2), and hydroxyl radical ($OH\bullet$), can directly damage the phospholipids within the cell membrane (Nadarajah et al., 2020), causing an increased permeability that can severely affect cellular integrity.

Plants have evolved a suite of sophisticated biochemical and physiological defense mechanisms, as well as specialized organizational structures, to combat salt stress. These adaptations include osmoregulation, reactive oxygen species (ROS) scavenging, effluence, sequestration and storage of

 doi:10.20944/preprints202410.1786.v1

toxic ions, and photosynthesis. For instance, the accumulation of specific amounts of inorganic ions or organic solutes can enhance the osmoregulatory capacity in plants, such as chrysanthemum (Li et al., 2022), potato (Sanwal et al., 2022), and rhododendron (Hou et al., 2021). Additionally, the activity of various antioxidant enzymes, including superoxide dismutase (SOD), peroxidase (POD), catalase (CAT), ascorbate peroxidase (APX), and glutathione reductase (GR), increases in plants to neutralize excess ROS (Zeeshan et al., 2020). It has been documented that the plasma membrane Na^+/H^+ transporter protein, known as salt overly sensitive 1 (SOS1), is instrumental in the efflux of Na^+. A loss-of-function mutant of rice lacking SOS1 exhibits heightened sensitivity to salt stress (El Mah et al., 2019). Furthermore, the vacuolar membrane Na^+/H^+ antiporter (NHX) plays a pivotal role in sequestering excess intracellular Na^+ into the vacuoles, thereby establishing ionic homeostasis (Liu et al., 2017; Long et al., 2020). Under salt stress, salt-tolerant potatoes can sustain a high K^+/Na^+ ratio, improved photosynthetic activity, and elevated levels of osmotic regulators and increased activity of antioxidant enzymes, which are crucial for their resilience to salt stress (Sanwal et al., 2022). Furthermore, throughout the long-term process of evolution, changes in the morphological structures of plants have become an essential pathway to adapt to unfavorable environments. For example, quinoa can sequester Na^+ into the epidermal bladder cells (EBCs) of old leaves as a defense against salt stress (Kiani-Pouya et al., 2017); similarly, *Limonium bicolor* possesses salt glands that can secrete excess salt from tissues to the outside of cells (Li et al., 2020). On the other hand, some organizational structures of plants also change in response to salt stress. For instance, stomatal density, as well as the development of palisade and spongy parenchyma, can be significantly increased to maintain plant photosynthesis under salinity (de Oliveira et al., 2019). Salt-tolerant proso millet (ST47) exhibits higher structural integrity with thicker cell walls in the root system, which act as barriers to prevent Na^+ entry, thus sustaining plant growth (Yuan et al., 2021). These adaptive mechanisms enable plants to resist adversity and maintain growth.

Sunflowers, recognized as a medium salt-tolerant crop (Taher et al., 2018), are among the world's most important economic oil crops, alongside soybeans, palm oil, and rapeseed (Bakhoum et al., 2020). However, research on the salt tolerance mechanisms in sunflowers is lacking. This study is dedicated to exploring the physiological mechanisms of salt tolerance by examining four sunflower germplasms—two salt tolerant genotypes (182265 and 182283) and two salt-sensitive ones (182093 and 186096)—during their seedling stage. The findings are expected to contribute significantly to the understanding of the molecular basis of salt tolerance in sunflowers and may help expedite the development of sunflower varieties with enhanced resilience to saline conditions.

Materials and Methods

Plant Materials, Growing Conditions, and Salt Stress Treatment

The seeds of oil sunflower germplasms, including the salt-tolerant genotype 182265 and 182283, and the salt-sensitive ones 182093 and 186096 (Li et al., 2020), were sourced from the Institute of Economic Crops, Xinjiang Academy of Agricultural Sciences. They were sown in a nutrient soil mix (perlite: vermiculite: floral soil = 1:1:3 by volume). The seedlings were cultivated in a greenhouse under a photoperiod of 16 hours light and 8 hours darkness at a temperature of 26°C (±2°C). Ten-day-old seedlings were subjected to a gradient salt stress with 350 mM NaCl, where the NaCl concentration was increased by 100 mM every 5 hours, culminating in a final addition of 150 mM. This treatment of 350 mM NaCl was applied for 4 days to observe the stressed phenotypes, analyze leaf anatomical structures, and measure physiological indices. Fresh samples were collected for the determination of photosynthetic parameters and for the staining of reactive oxygen species (ROS). Following 24 hours of salt stress, samples of roots and leaves, with three biological replicates each, were collected separately, quickly frozen in liquid nitrogen, and stored at -80°C for subsequent analysis of quantitative real-time PCR (qRT-PCR).

Root System Scanning and Basic Analysis

 doi:10.20944/preprints202410.1786.v1

The root systems' appearance was scanned, and their root lengths were measured using a Win RHIZO 2020 scanner from Régent Instruments Inc. It is important to note that the cleaned and intact root systems were placed in a background tank containing distilled water. The roots were carefully arranged to ensure that lateral roots were fully extended, minimizing the occurrence of crossing over.

Measurements of Chlorophyll Content and Various Photosynthetic Indices

Chlorophyll content was determined using the trace method (Arnon, 1949). 0.1 g fresh first pair of true leaves removing veins, were ground into powder in liquid nitrogen. Subsequently, the samples were mixed with 10 mL of reaction solution containing 80% acetone and 95% alcohol (v: v = 1: 1) and incubated for 24 hours at 25°C in the dark until the leaves turned colorless. The absorbance of the samples was measured at wavelengths of 663, 645, and 470 nm using a UV-visible spectrophotoometer (UV-2600, Shimadzu, Japan).

True leaves were used to measure photosynthetic parameters, including the photosynthetic rate, stomatal conductance, water use efficiency, and intercellular CO2 concentration. These measurements commenced at 12:00 noon following 4 days of salt stress, utilizing a CIRAS-3 Portable Photosynthesis System (PP Systems, USA). The cuvette was maintained in an environment with a photosynthetic photon flux density (PPFD) of 1000 μmol/m²/s and a relative humidity of 70%.

Leaf Anatomical Structures

Samples from the middle part of the true leaf were fixed in FAA fixative for 24 hours. Subsequently, the leaf tissues were dehydrated through an alcohol gradient, rom low to high concentrations of 70%, 80%, 90%, 95%, 100% (Periasamy et al., 1967). And then, the samples were then embedded in wax and sectioned into 10-12 μm thick slices using a semi-automatic microtome (Leica RM2125 RTS, Nussloch, Germany). After dewaxing, the sections were stained with safranin O and counterstained with fast green. After sealing with neutral gum, the sections were examined under a light microscope at a magnification of ×100.

Detection of EL, MDA, H_2O_2, and O_2^-

Electrolyte leakage (EL) was measured using a conductivity meter (DSS, China) (Zhang et al., 2012). Initially, leaves or roots (approximately 5 g fresh weight) were immersed in centrifuge tubes containing 30 mL of ultrapure water for 24 hours. Subsequently, the conductivity of the solution was measured once, with the value denoted as E1. Following this, the tissues in the centrifuge tubes were boiled for 1 hour, and the resulting value was designated as E2. The electrolyte leakage rate was calculated using the formula E1/E2×100%.

MDA content (μmol/g FW) was determined according to this method (Spitz et al., 1989) with the handy and commercial kit (Solarbio, BC0025). 0.1 g roots or leaves were ground into powder in liquid nitrogen. The powder was dissolved in phosphate buffer solution (pH 7.8) and the solution was centrifuged to obtain supernatant. And then, supernatant was mixed with 0.5% trichloroacetic acid (TCA) containing 0.5% thiobarbituric acid (TBA) and boiled in a water bath for 1 h. After cooling, the absorbance was determined at wavelengths of 532 and 600 nm.

H_2O_2 content (μmol/g FW) was measured according to this documentary (Satterfield et al., 1955; Amin et al., 1967) and following the manufacturer's instructions (Solarbio, BC3595). 0.1 g tissues was homogenized in acetone on an ice bath, and the supernatant was obtained by centrifugation. H_2O_2 in the supernatant reacted with 0.1% titanium sulfate dissolved in 20% H_2SO_4 to form a yellow titanium peroxide complex. The absorbance was measured at 415 nm.

O_2^- content (μmol/g FW) was measured based on this principle (Cai et al., 2017) with the commercial kit (Solarbio, BC1295). The supernatant prepared by the same method as for MDA was mixed with hydroxylamine hydrochloride reagent to react; and then, aminobenzenesulfonamide and naphthalene ethylenediamine hydrochloride were added to the mixture to produce a purplish-red azo compound. Finally, chloroform was added for extraction, and the upper aqueous phase obtained by pumping was determined as a characteristic absorption peak at 530 nm.

 doi:10.20944/preprints202410.1786.v1

For ROS staining, the true leaves were soaked in a solution containing 1 mg/mL of DAB, NBT, and Evans blue at 37°C in the dark for 24 hours. Subsequently, the leaves were placed in absolute alcohol and boiled in a water bath to remove chlorophyll.

Measurement of Various Antioxidant Enzyme Activities

For determination of antioxidant enzymes, about 0.1 g root or leaf tissue was homogenized with PBS buffer (pH 7.8, 0.1 M) in an ice bath, and centrifuged at 8000 rpm/min for 10 min at 4°C to obtain the supernatant, which was used to determine the activities of SOD, POD, CAT, APX, GR, T-AOC. They were measured by following the manufacturer's instructions (Solarbio, BC0175, BC0095, BC0205, BC0225, BC1165, BC1315).

The SOD (EC 1.15.1.1) activity (U/g FW) was assayed by photochemical reduction of nitrogen blue tetrazolium (NBT) (Giannopolitis et al., 1977; Agarwal et al., 2004). Under the presence of methionine and riboflavin, NBT undergoes a photochemical reduction reaction upon exposure to light, resulting in the formation of blue methylhydrazine. SOD can inhibit the photochemical reduction of NBT, and its inhibition intensity is proportional to the enzyme activity within a certain range. The blue methylhydrazine exhibits maximum light absorption at 560 nm.

The POD (EC 1.11.1.7) activity (U/g FW) was carried out using the guaiacol method (Reuveni et al., 1992; Doerge et al., 1997). The supernatant was mixed with 3,3-diaminobenzidine-tetrahydrochloride dihydrate (DAB), 50% (w/v) gelatin, 0.6% H_2O_2, and distilled water. POD in the presence of H_2O_2 oxidized guaiacol to produce tetra-o-methoxyphenol (a tea-brown substance), which had a light-absorption peak at 470 nm.

The CAT (EC 1.11.1.6) activity (U/g FW) was determined following the method (Johansson et al., 1988). The supernatant was incubated with a working solution consisting of 3% hydrogen peroxide (H_2O_2) and 0.1 mM EDTA. CAT enzyme activity was calculated by measuring the amount of CAT-catalyzed decomposition of H_2O_2 over a certain period of time. H_2O_2 showed a characteristic absorption peak at 240 nm.

The APX (EC.1.11.1.11) activity (U/g FW) was measured following the principle (Shigeoka et al., 1980; Caverzan et al., 2012). The supernatant was mixed with a working solution consisting of 0.5 mM ascorbic acid (AsA), 0.1 mM EDTA, 0.1 mM H_2O_2. The oxidation of AsA by H_2O_2 requires APX as a catalyst. APX activity was calculated by measuring the amount of catalytically decomposed AsA over a certain period of time. AsA showed a characteristic absorption peak at 290 nm.

The GR (EC1.8.1.7) activity (U/g FW) was measured by Demiral's description (2005). The supernatant was mixed with 0.5 mM GSSG and 0.12 mM NADPH-Na_4. GR catalyzes the reduction of GSSG by NADPH and the regeneration of GSH, and the dehydrogenation of NADPH to $NADP^+$; NADPH has a characteristic absorption peak at 340 nm.

The T-AOC activity (U/g FW) was measured based on the method (Benzie and Strain, 1996). The antioxidant substances in the extraction reacted with Fe^{3+}-tripyridyltriacridazine (Fe^{3+}-TPTZ), generating blue Fe^{2+}-TPTZ. Fe^{2+}-TPTZ was proportional to the total antioxidant capacity and it showed a characteristic absorption peak at 593 nm.

Determination of Compatible Osmolytes

The detection methods for the osmoregulatory substances, including proline, soluble sugars, and soluble proteins were as follows with the commercial kit (Solarbio, BC0255, BC0035, PC0020).

The proline content (μg/g) was based on the ninhydrin method (Demiral et al., 2005). Proline was extracted from tissues using sulfosalicylic acid. The supernatant was mixed with ninhydrin reagent and glacial acetic acid heated in boiling water at 100 ℃ for 30 min, and the solution became red in colour. Then the red pigment was extracted with toluene and then the absorbance was measured at 520 nm.

The soluble sugar content (mg/g) was determined using the anthrone colorimetric method (Buysse et al., 1993; Bodelón et al., 2010). 0.1 g of homogenate was obtained by grinding root or leaf tissues with distilled water. It was heated in a water bath for 10 min, cooled, and centrifuged to obtain the supernatant. The supernatant was mixed with anthrone and concentrated sulfuric acid (H_2SO_4),

 doi:10.20944/preprints202410.1786.v1

heated in a water bath for 10 min, resulting in the production of furfural derivatives with an absorption peak at 620 nm.

The soluble protein content (mg/g) was determined according to the method (Sedmak et al., 1977; Scopes et al., 1987). The supernatant was obtained in the same way as antioxidant enzymes. Under alkaline conditions, the protein in the supernatant can reduce Cu^{2+} to Cu^{+}, Cu^{+} and bicinchoninic acid (BCA) reagent form a violet-blue complex（two molecules of BCA can chelate into a Cu^{+}）with an peak absorption at 562 nm.

Detection of Na^{+} and K^{+} Contents

leaves or roots were first oven-dried at 80°C to a constant weight. The dried samples were then ground into a fine powder and 40-mesh sieve was used to eliminate large particles. 0.3 g powdered sample was ashed in a crucible at 560°C for 5 hours and after ashing, 1.5 mL H_2SO_4 was added to the crucible to dissolve the ash completely. The Na^{+} and K^{+} contents of the dissolved ash were then measured using a flame photometer (AP1500, China). The entire experiment was performed by Jiangsu Addison Biotechnology Co., Ltd., China.

Analysis of Gene Expression by Quantitative Real-Time Polymerase Chain Reaction

Total RNA was extracted with sunflower leaves or roots utilizing the Plant RNA Kit (Omega BioTek, USA), and the RNA samples were treated with DNase I to preclude any genomic DNA contamination. RNA was reverse-transcribed to cDNA by SuperScript™II Reverse Transcriptase (Takara, Japan) and oligo(dT)$_{18}$ primers. Quantitative gene expression analysis was performed using the CFX96 Rapid Real-Time PCR Detection System (Bio-Rad, USA). *HaActin* and *HaEF-1* were employed as internal references. The relative expression levels of the genes were calculated using the $2^{-\Delta\Delta CT}$ comparison method. Each sample set was composed of three biological replicates and two technical replicates to ensure the reliability and reproducibility of the results. Details of the primers used in this study were provided in Supplementary Table S1.

Statistical Analysis

The statistical analyses for our studys were performed using SPSS Statistics Software (version 19, IBM). Multifactorial Analysis of Variance (ANOVA) was the primary method employed to discern differences among various groups, including all germplasm controls and treatments. Each sample was represented by a minimum of three biological replicates, and subsequent mean comparisons were made using Dunnett's test at a significance level of $p \leq 0.05$. Student's t-tests were applied to compare the differences in the ion content or gene expression between individual controls and treatments for each germplasm. For gene expression analysis, each gene was examined with three biological replicates and two technical replicates to ensure the robustness of our findings. Post hoc Duncan's multiple comparisons tests were applied to delineate significant differences at various levels:*p<0.05, **0.05<p<0.01, ***0.001<p<0.01, ****p<0.001. All data were expressed as the mean±standard deviation (mean±SD). GraphPad Prism 5 software was utilized to plot the data. Additionally, principal component analysis (PCA) was conducted to perform multivariate analyses on all parameters for the four oil sunflower genotypes under both control and salt stress conditions, providing a comprehensive view of the data structure. ImageJ was employed to quantify relevant data extracted from images.

Results

The Above-Ground and Below-Ground Morphological Phenotypes of Four Sunflower Germplasms Under Salt Stress

Based on an evaluation of the salt tolerance among nearly 600 oil sunflower germplasms during the germination stage (Li et al., 2020), we identified the most salt-tolerant germplasms, 182265 and

 doi:10.20944/preprints202410.1786.v1

182283, as well as the most salt-sensitive ones, 182093 and 186096, for further investigation of their physiological responses to salt stress.

Under normal growth conditions, all seedlings displayed robust growth. After a 4-day exposure to 350 mM NaCl, the salt-tolerant genotypes 182265 and 182283 retained a healthy appearance with green leaves, smaller change in root contour, and a modest reduction in total root length (18.36% and 23.87%, respectively). In contrast, the salt-sensitive genotypes 182093 and 186096 showed more severe effects with wilted and yellowed leaves, marked alteration in root contour, and a significant reduction in total root length (53.12% and 52.66%, respectively), when

compared to their individual controls (**Figure 1A-C**). The phenotypic responses of both the above-ground and below-ground parts were congruent with the salt tolerance or sensitivity profiles of the respective germplasms.

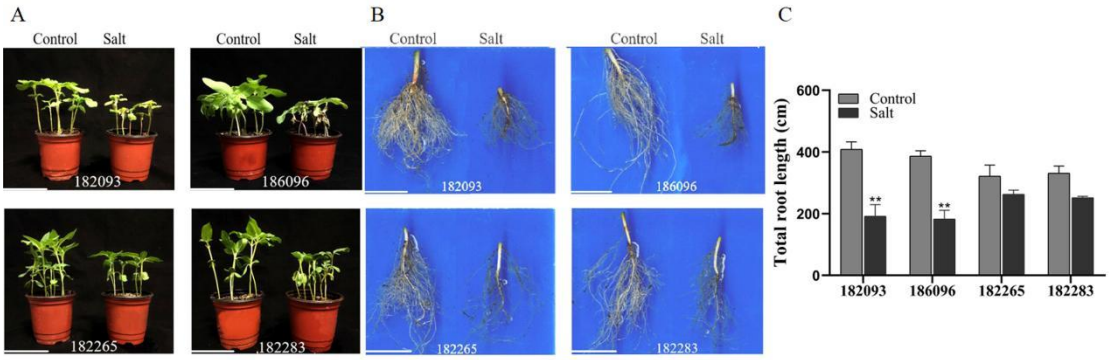

Figure 1. Morphological phenotypes of four sunflower germplasms under salt stress. Ten-day-old seedlings of the genotypes 182265, 182283, 182093, and 186096 were subjected to a 350 mM NaCl stress for a period of four days. A parallel set of seedlings were treated with distilled water as controls. (A) The above-ground phenotype; (B) root contour; (C) Total root length. The scale bars are marked at 10 cm. Significant differences between the control and salt-stressed seedlings of the same germplasm are denoted by asterisks (*), as determined by Duncan's multiple range test following a post hoc analysis. (*$P < 0.05$ and **$0.001 < P < 0.01$).

Effect of Salt Stress on Photosynthetic Characteristics and Leaf Structure in Sunflowers

The photosynthetic rate (PR), chlorophyll content (CC), stomatal conductance (SC), and water use efficiency (WUE) of four sunflower genotypes were compared under both control and salt stress conditions (**Figure 2A-D**). Under control conditions, there were no significant differences among genotypes 182265, 182283, 186096, and 182093 for most of these indices. However, under salt stress, genotype 182265 exhibited the highest values in all categories, being 82.79% (PR), 60.76% (CC), 59.06% (SC), and 70.90% (WUE) higher than genotype 182093; and 65.52% (PR), 26.59% (CC), 70.5% (SC), and 51.90% (WUE) higher than genotype 186096, respectively. Genotype 182283 followed, showing 81.18% (PR), 61.25% (CC), 37.18% (SC), and 66.91% (WUE) higher values than genotype 182093; and 69.13% (PR), 27.5% (CC), 54.75% (SC), and 45.31% (WUE) higher than genotype 186096. This suggests that the photosynthetic performance of salt-tolerant genotypes under salt stress is significantly superior to that of salt-sensitive genotypes.

The anatomic structures of the leaves from the most salt-tolerant (182265) and the most salt-sensitive (182093) sunflower genotypes were investigate under salt stress. Under control conditions, the spongy tissues were neatly arranged, and the vascular tissues were well-developed in the leaves of both contrasting sunflower genotypes. And the leaves of salt-sensitive resources were slightly thicker compared to salt-tolerant genotypes. Under salt stress, genotype 182093 showed a reduction in leaf thickness, with a 43.21% decrease in the spongy tissue area and an 18.55% decrease in the vascular tissue area, compared to the control; In contrast, genotype 182265 did not exhibit significant changes in either structure (**Figure 2E**). These findings indicate that efficient photosynthesis and an intact leaf tissue structure are essential for salt stress resistance in sunflowers.

 doi:10.20944/preprints202410.1786.v1

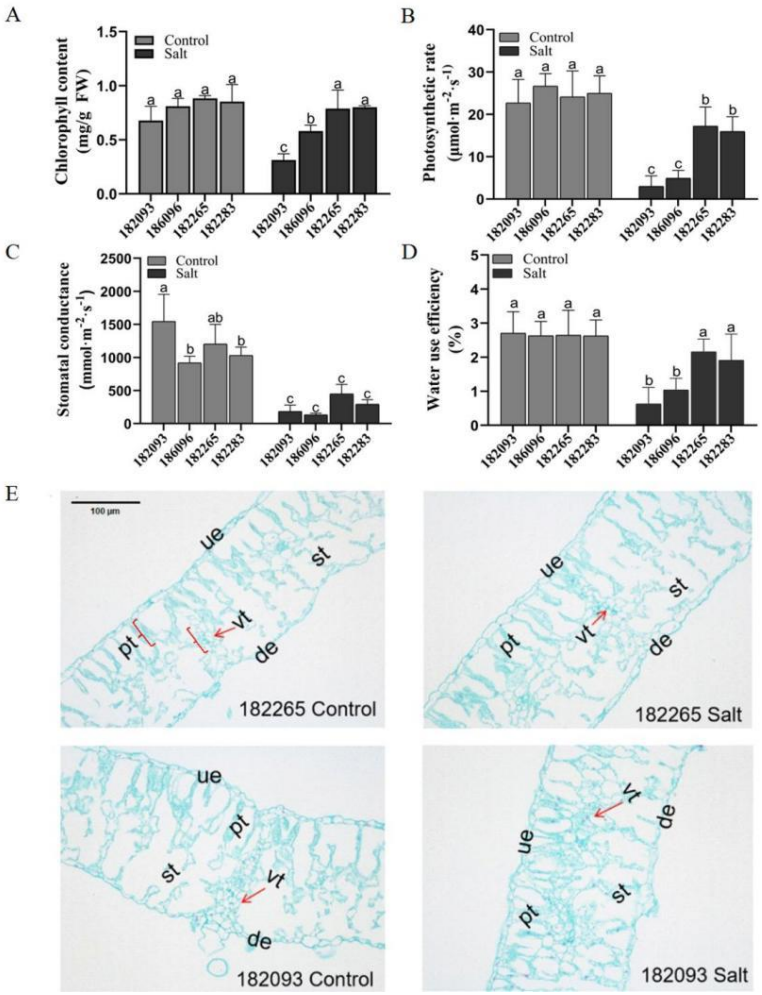

Figure 2. Comparative analysis of photosynthetic characteristics and leaf anatomical structures between salt-tolerant (182265) and salt-sensitive (182093) sunflower genotypes under salt stress. (A) Chlorophyll content; (B) Photosynthetic rate; (C) Stomatal conductance; (D) Water use efficiency. (E) Microscopic views of the leaf anatomical structures of genotypes 182265 and 182093. The images were captured at an original magnification of ×100. The anatomical features are labeled as follows: Ue, upper epidermis; de, lower epidermis; pt, palisade tissue; st, spongy tissue; vt, vascular tissue. Significant differences ($p \leq 0.05$) among all the samples of the four sunflower germplasms under both control and salt treatment were denoted by different letters.

Salt Stress on Damage to Cell Membrane of Sunflowers

Salt stress causes oxidative stress and membrane damage in plant cells. We detected oxidative levels based on DAB and NBT staining (**Figure 3A and B**), the contents of H_2O_2 (**Figure 3F-G**) and O_2^- (**Figure 3H-I**); and cell membrane damage were detected by Evans blue staining (**Figure 3C**), the determination of MDA (**Figure 3D and E**) and EL (**Figure 3J-K**). The results showed, in the four sunflower resources, the cell membrane damage and the accumulation of reactive oxygen species (ROS) in the roots were significantly higher than in the leaves (**Figure 3D-K**). Specifically, the average levels of malondialdehyde (MDA), electrolyte leakage (EL), hydrogen peroxide (H_2O_2), and superoxide anion (O_2^-) in the roots of the two salt-tolerant genotypes were 34.21%, 34.28%, 47.12%, and 35.64% lower, respectively, than those of the salt-sensitive genotypes (**Figure 3E, G, I, K**). Likewise, in the leaf tissues, these differences between the salt-tolerant and sensitive genotypes were reduced, with reductions of 29.09%, 36.02%, 28.87%, and 36.25%, respectively (**Figure 3D, F, H, J**). These results indicated that the salt-tolerant genotypes accumulated less ROS

 doi:10.20944/preprints202410.1786.v1

in their tissues and had a lower degree of cell membrane damage, which may be one of the reasons for their higher tolerance to salt stress.

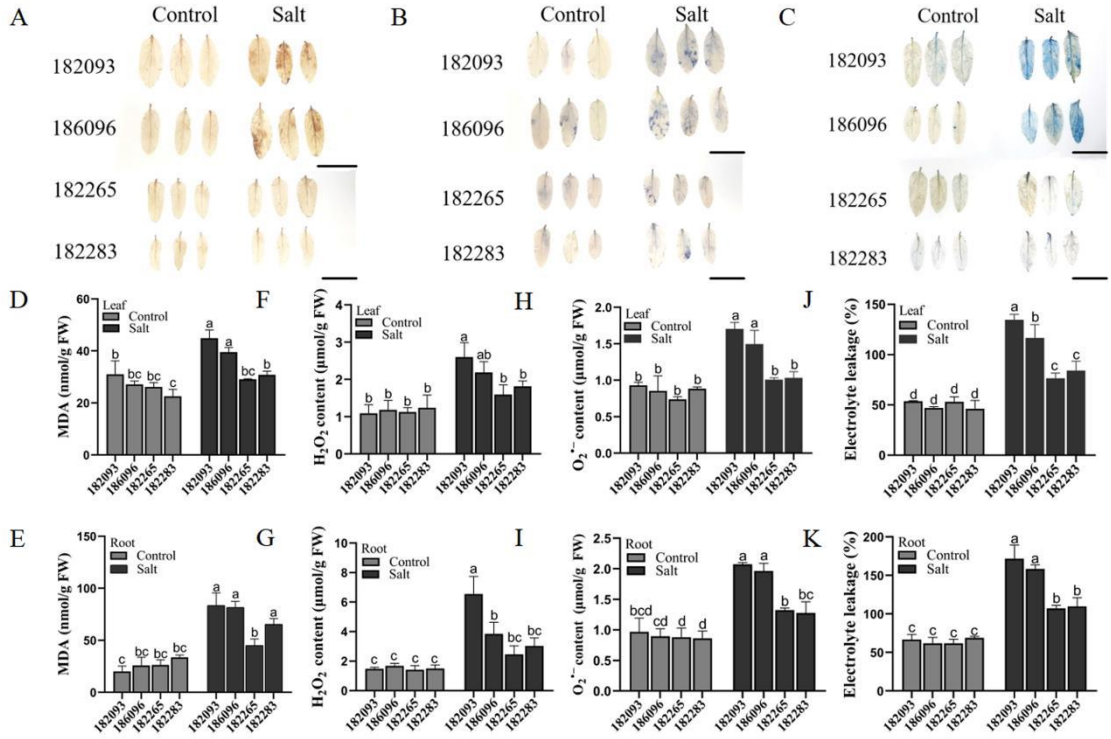

Figure 3. Comparative cell membrane damage in salt-tolerant and salt-sensitive Sunflower germplasms under salt stress. (A-C) Histochemical staining for cellular damage using DAB, NBT, and Evans blue in the leaves and roots, respectively. (D-K) Quantitative analysis of MDA, H_2O_2, and O_2^- contents, and electrolyte leakage rate in the leaves and roots of four sunflower germplasms. The scale bars represented 5 cm. Different letters denoted significant differences among all the samples of the germplasms in control and treatment with 350 mM NaCl for 4 days ($p \leq 0.05$).

Improved Activityes of Antioxidant Enzymes for ROS Scavenging in Salt-Tolerant Germplasms

To determine whether enzyme activities are different between salt-tolerant and salt-sensitive sunflowers under salt stress, we assayed the antioxidant enzyme activities of POD, SOD, CAT, APX, and GR and total antioxidant capacity (T-AOC) in leaves and roots of the four sunflower germplasms (**Figure 4A-H**). The results showed that the mean values of five enzymes activities (SOD, POD, CAT, APX and GR) in the different tissues of the two salt-tolerant resources 182265 and 182283 were higher than those in the salt-sensitive resources 182093 and 186096 by 34.89%, 38.8%, 36.08%, 19.66%, 46.69% (in roots), 28.03%, 43.7%, 43.71%, 41.93%, and 43.48% (in leaves) (**Figure 4A-J**). In addition, the antioxidant enzyme activities in the leaves of sunflower from all resources were less than roots; for example, in 182265, CAT, APX and GR enzyme activities reached 135.06 U/g, 6.76 U/g and 0.63 U/g in roots and 101.41 U/g, 3.8 U/g and 0.497 U/g in leaves, respectively (**Figure 4E-J**). The determination of total antioxidant capacity test (T-AOC) showed that antioxidant capacity 182265 was the strongest and 182093 was the weakest (**Figure 4K-L**). These results suggest that salt tolerant sunflower improves tolerance to salt stress by enhancing the activity of antioxidant enzymes; and the enzyme activity was higher in roots than leaves.

 doi:10.20944/preprints202410.1786.v1

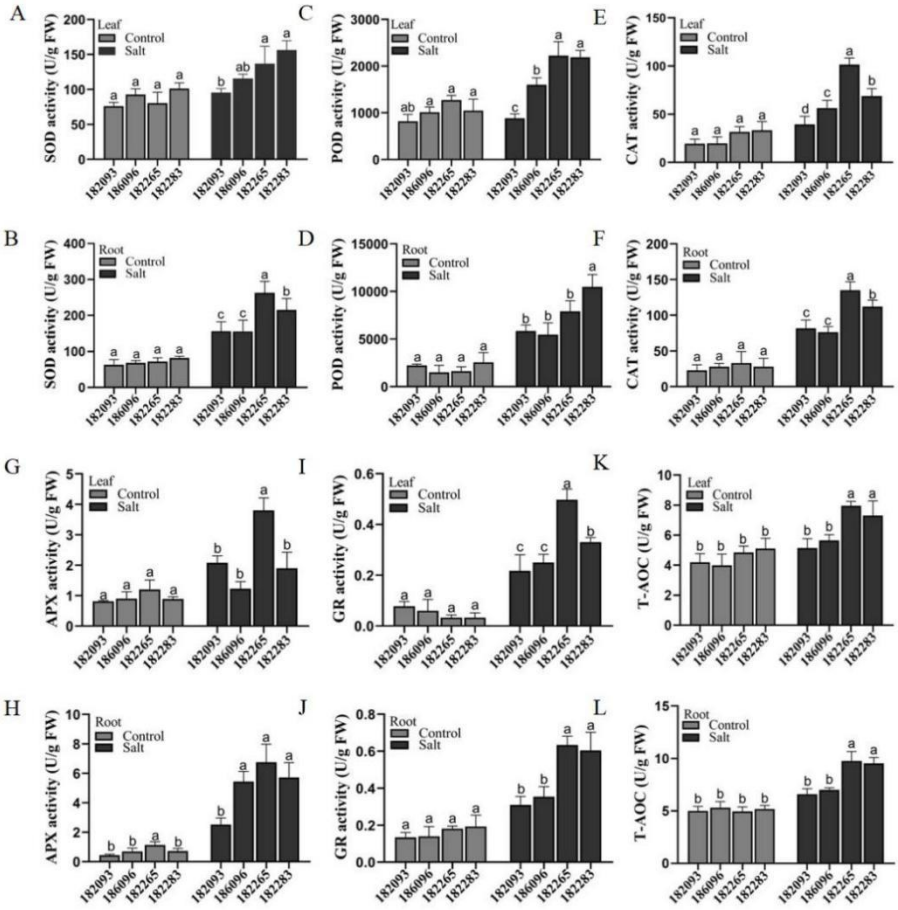

Figure 4. Antioxidant enzyme activities in salt-tolerant and salt-sensitive sunflower germplasms. (A-L) The activities of SOD, POD, CAT, APX, GR, and the T-AOC in both leaves and roots. Data were presented as the mean of three biological replicates. Different letters indicated significant differences among all the samples of the four germplasms in controls and treatments with 350 mM NaCl for 4 days ($p \leq 0.05$).

Enhanced Osmoregulatory Capacity by Accumulating Compatible Osmolytes in Salt-Tolerant Germplasms

The accumulation of compatible osmotic solutes, such as proline, soluble sugars, and soluble proteins, serves as a critical mechanism for enhancing salt tolerance in plants. In an analysis of four sunflower genotypes, it was observed that salt stress induced an average increase in proline content of 34.93% in leaves and 36.42% in roots for the salt-tolerant genotypes 182265 and 182283, compared to the salt sensitive genotypes 182093 and 186096 (**Figure 5A and B**). The levels of soluble sugars and soluble proteins mirrored the trend observed for proline (**Figure 5C-F**). The average contents of soluble sugars, and soluble proteins in differen tissues of the two salt-tolerant genotypes 182265 and 182283 were 49.49%, 37.98%（in roots）, 35.75% and 26.34% (in leaves) higher than those in the salt-sensitive genotypes 186096 and 182093). Indeed, in salt-tolerant plants, a significant accumulation of osmolytes can significantly accumulate in salt-tolerant sunflowers in response to salt stress.

 doi:10.20944/preprints202410.1786.v1

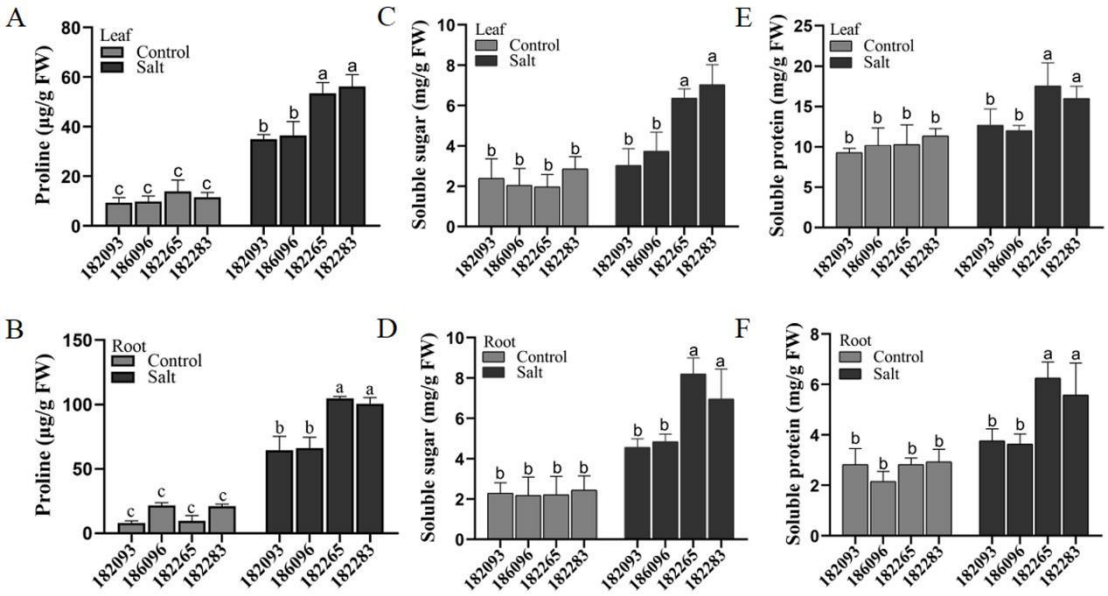

Figure 5. Comparison of the accumulation of various compatible osmolytes in the leaves and roots of salt-tolerant and salt-sensitive sunflower germplasms. The contents of proline (A-B), soluble sugars (C-D), and soluble proteins (E-F) in the leaves and roots were shown. The data represented the average of three biological replicates. Different letters indicated significant differences among all samples of the four germplasms under control conditions and treatments with 350 mM NaCl for 4 days ($p \leq 0.05$).

Salt Tolerant Sunflower Germplasm Having the Ability with Enhanced Na^+ Exclusion and K^+ Uptake in Roots and Leaves

It is widely recognized that excessive Na^+ can be detrimental to plants, while K^+ are essential for their growth and development (Zhao et al., 2020). In our study, we compared the most salt-tolerant sunflower genotype (182265) with the most salt-sensitive genotype (182093) to determine the contents of Na^+ and K^+ in the leaves and roots. Under control conditions, there was no significant difference in the levels of these ions between the two genotypes. However, under salt stress, genotype 182265 exhibited a markedly reduced accumulation of Na^+ and maintained higher K^+ levels in both roots and leaves compared to genotype 182093 (**Figure 6A-D**). Consequently, the Na^+/K^+ ratios in the salt-tolerant genotype 182265 were significantly lower than those in the salt-sensitive genotype 182093 (**Figure 6E and F**). These findings suggest that salt-tolerant sunflower germplasm possesses the ability to regulate ion concentrations, specifically by accumulating lower levels of Na^+ and higher levels of K^+ in its roots and leaves, which may be a crucial adaptation mechanism for thriving in saline conditions.

 doi:10.20944/preprints202410.1786.v1

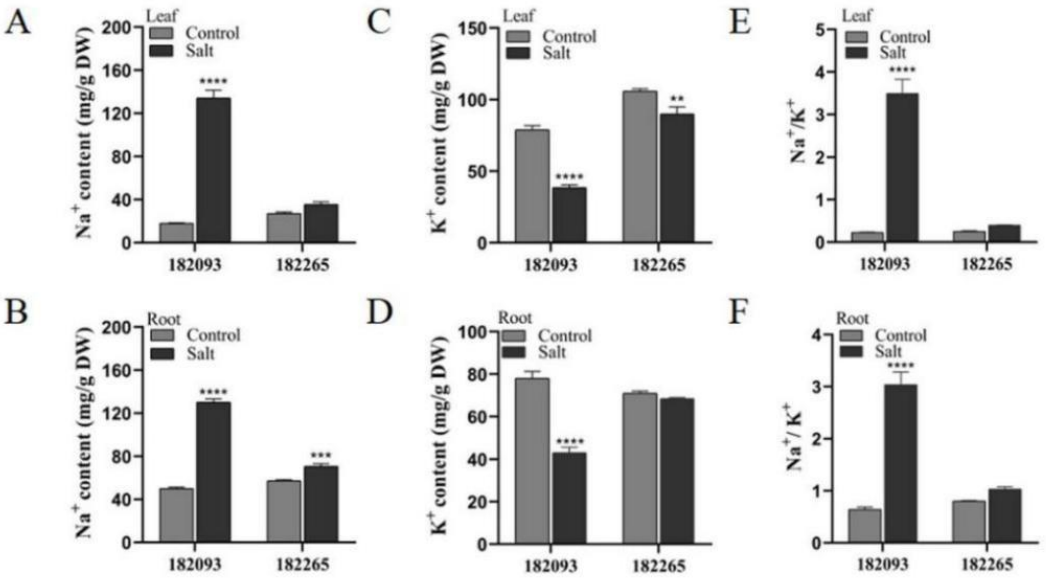

Figure 6. Assessment of ionic homeostasis in salt-tolerant and salt-sensitive sunflower genotypes under salt stress. The figure depicted comparative levels of Na^+ (A-B), K^+ (C-D), and the ratios of Na^+/K^+ (E-F) in the leaves and roots of the respective sunflower genotypes. Distinct asterisks (*) denoted statistically significant differences between control and salt-stressed conditions for each germplasm, as determined by post hoc Duncan's multiple comparisons tests (*p<0.05, **0.05<p<0.01, ***0.001<p<0.01, ****p<0.001).

The Expressions Analysis on Various Kinds Genes in Sunflower Under Salt Stress

The expression of the osmotic regulation gene *HaP5CS*, ROS clearance genes *HaPOD2* and *HaCAT1*, Na^+/H^+ antiporter genes *HaNHX* and *HaSOS* and stress-responsive gene *HaRD29A* and ABA synthesis key enzyme gene *HaNCED3* was evaluated in salt-tolerant and sensitive germplasms 182265, 182093 (**Figure 7**). qRT-PCR assays indicated that exposure to 350 mM NaCl for 24 hours induced the expression of the majority of the tested genes. In salt tolerant genotype 182265, the expression of *HaSOS1*, *HaSOS2*, and *HaSOS3* was approximately 2.4, 7.5, and 6.3 folds higher in the leaves, respectively, and approximately 18.8, 17.43, and 7.6 folds higher in the roots compared to the control. The upregulation of these genes was significantly greater in 182265 than in the salt-sensitive genotype 182093 (**Figure 7G-L**). This suggests that salt-tolerant sunflower has a strong capacity to exclude Na^+ to the extracellular space.

The expression of the vacuolar membrane Na^+/H^+ antiporter genes *HaNHX1* and *HaNHX2* were also significantly upregulated in both leaves and roots of genotype 182265 under salt treatment, with increases of 1.43, 3.07 times (in leaves), 3.91, 2.55 times (in roots), respectively, compared to the genotype 182093 (**Figure 7M-P**). Furthermore, the expression of *HaP5CS*, *HaPOD2*, and *HaCAT1* was significantly higher in genotype 182265 than in genotype 182093 (**Figure 7A-F**), which was consistent with the results of the physiological assays. The expressions of another two genes *HaRD29A* and *HaNCED3* were also significantly higher in genotype 182265 than 182093. These findings suggested that salt-tolerant sunflowers exhibited salt tolerance through the combined action of plasma membrane and vacuolar membrane Na^+/H^+ antiporters, the accumulation of osmoregulatory

 doi:10.20944/preprints202410.1786.v1

substances, and the increased activities of antioxidant enzymes as well.

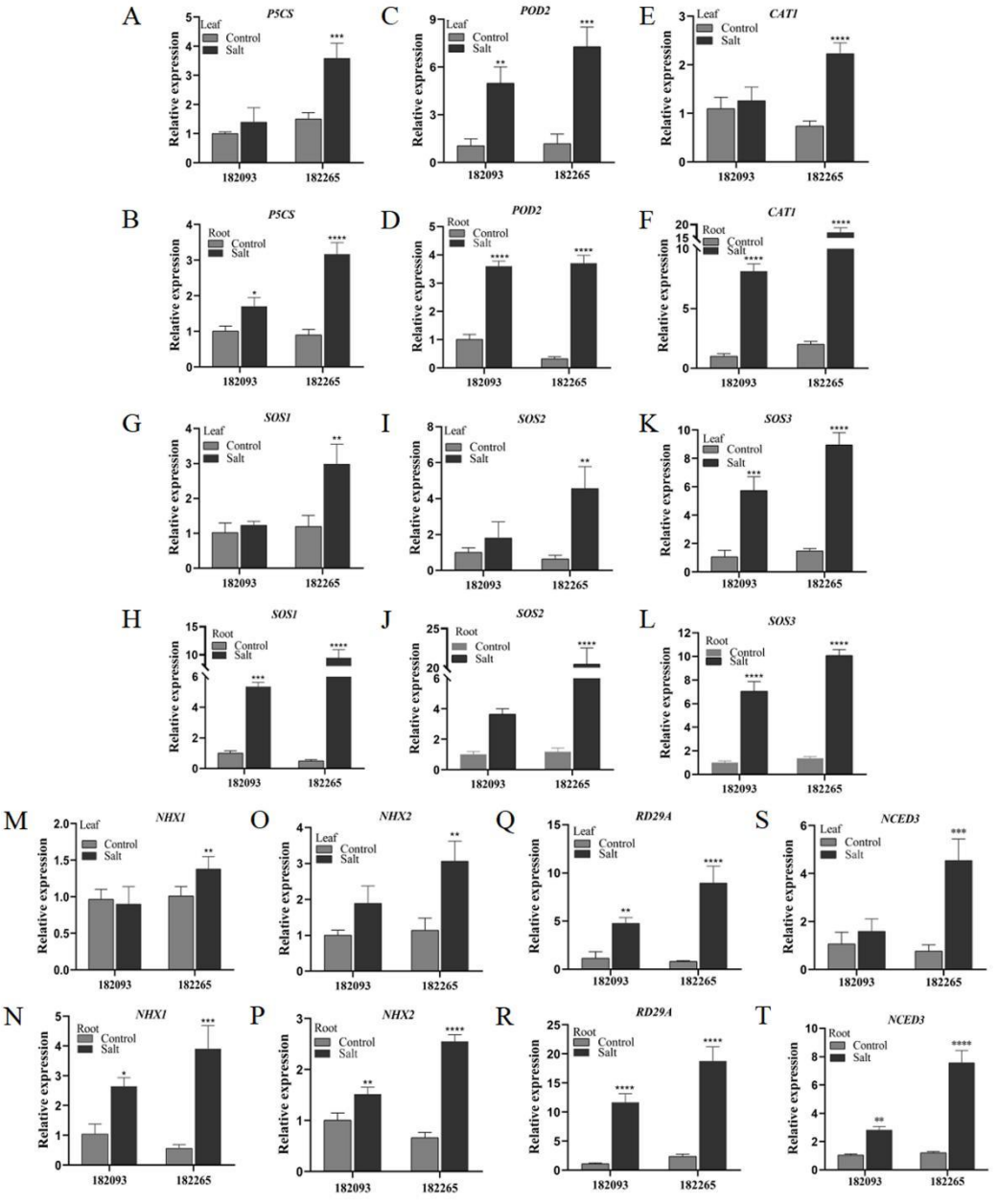

Figure 7. Expression analysis of various genes related to osmotic regulation, ROS clearance, and stress response in salt-tolerant and sensitive sunflower genotypes 182265 and 182093 under salt stress. The expression levels of the osmotic regulation gene *HaP5CS* (A-B), antioxidant enzyme genes *HaPOD2* and *HaCAT1* (C-F), plasma membrane Na^+/H^+ antiporter genes *HaSOS1*, *HaSOS2*, and HaSOS3 (G-L), vacuolar membrane Na^+/H^+ antiporter genes *HaNHX1* and *HaNHX2* (M-P), stress-responsive gene HaRD29A (Q-R), and the ABA synthesis key enzyme gene *HaNCED3* (S-T) in the leaves and roots of genotypes 182265 and 182093 were depicted. Asterisks (*) denoted significant differences between control and salt treatment within the same germplasm (*p<0.05, **0.05<p<0.01, ***0.001<p<0.01, ****p<0.001).

Principal Component Analysis (PCA) with the Data of Above All Physiological Indices

As we are well-known sunflower exerting salt tolerance is the result of a combination of multiple physiological and biochemical indices. Principal component analysis (PCA) was used to understand the response of physiological indices to salt stress, and to comprehensively compare the differences in different genotypes. In this study, the physiological data were distinguished into two principal

 doi:10.20944/preprints202410.1786.v1

components (PC), PC1 and PC2, and the contribution rates of PC1 and PC2 to the entire variable were 62.905% and 32.978%, respectively, with greater eigenvalues than 1 selected. the cumulative contribution rate of the first two PCs was 95.883% (**Figure 8A**). The plot component weights are shown in Figure 8A. The index that contributed most to PC1 (62.905%) were GR, followed by SS, NaK, AOC, CAT, APX, and Na, while the maximum contribution indicators in PC2 (32.978%) were SP, POD, MDA and H_2O_2 (**Figure 8A**). The physiological responses of different genotypes under different treatment conditions were evaluated by PCA (**Figure 8B**). The difference in the physiological status of individual genotypes under control was small. However, different genotypes were clearly separated after salt treatment. The physiological salt tolerance of the four genotypes was proved to be in the order: 182265 > 182283 > 186096 > 182093 (**Figure 8**), when the biochemical indices were tested using roots and leaves as materials, respectively. This was consistent with the above experimental phenotype. Additionally, the difference in the physiological responses of roots was larger than those of the leaves among the genotypes. This occurred probably because Roots came into direct contact with salt solution.

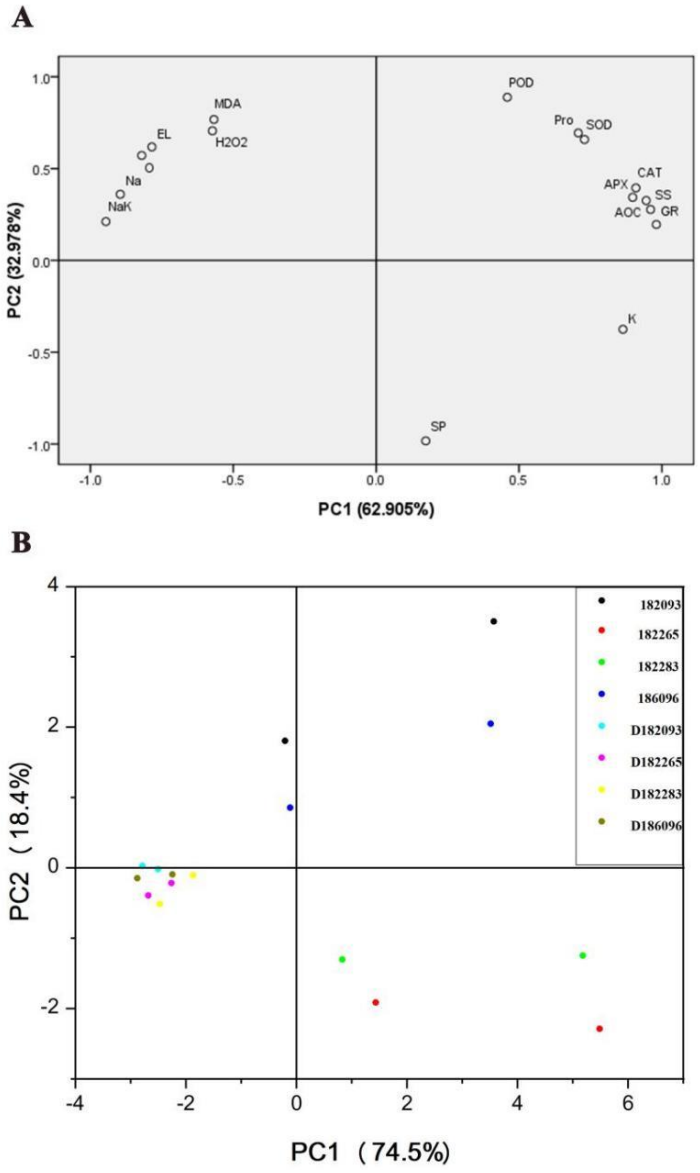

Figure 8. Principal component analysis (PCA) was conducted on the physiological state and different genotypes during salt stress, based on the data of various physiological indicators. (A) PCA of physiological indicators under salt stress. (B) PCA of the differences among genotypes. SP: Soluble protein; SS: Soluble sugar; Pro: Proline; K: K^+; Na: Na^+; NaK: Na^+/K^+; APX: APX activity; CAT: CAT

 doi:10.20944/preprints202410.1786.v1

activity; GR: GR activity; POD: POD activity; SOD: SOD activity; AOC: T-AOC; O: O_2^- content; EL: Electrolyte leakage; H_2O_2: H_2O_2 content; 186096, 182093, 182283, and 182265: genotypes in the 350 mM NaCl treatment group. D186096, D182093, D182283, and D182265: genotypes in the control group. The dots of the same colour are the root and leaf of the same resource.

Discussion

Strong Photosynthetic Ability is Closely Related to the Tissue Structure on Salt Tolerance in Sunflowers

Photosynthesis is essential for plant growth and development. Salt stress destroys chloroplast structure and reduces chlorophyll content, which adversely affects the bioenergetic process of photosynthesis (Jiang et al., 2021; Li et al., 2019). We assessed the salt tolerance of different genotypes in sunflower using photosynthesis-related metrics, such as chlorophyll content, photosynthetic rate, stomatal conductance and water use efficiency. It found that the chlorophyll contents of salt-tolerant germplasms 182265 and 182283 in leaves were not significantly different under salt stress, whereas they were significantly decreased in salt-sensitive germplasms 182093, 186096 (**Figure 2A**). In addition, other some photosynthesis-related indexes of photosynthetic rate, stomatal conductance and water use efficiency have similar trends between salt-tolerant and sensitive germplasms (**Figure 2B-D**). Some literature reports also supported our results (Shokoofeh et al., 2021; Elvany et al., 2022). Secondly, high salinity also alters the leaf tissue structure and hence affected photosynthesis in plants. *Populus talassica* × poplar (*Populus talassica* × *P. euphratica*) is a more salt-tolerant hybrid, with structurally intact and thickened leaf palisade tissue under salt stress (Liu et al., 2022); seawater-stressed wheat were dwarfed and the vascular area of the leaves was reduced (Nassar et al., 2020); similar results also have been shown in amaranth (*Amaranthus caudatus* L.) (Estrada et al., 2021) and kala grass (*Leptochloa fusca* L.) (Abd-Elbar et al., 2012). In our study, leaf structure in salt-tolerant germplasm 182265 remained unchanged under salt stress, while there were a reduced area of spongy and vascular tissues in salt-sensitive germplasm 182093 (**Figure 2E**). These indicated that salt tolerance in sunflower is correlated with intact leaf structure and maintenance of good photosynthesis.

Enhancing the Activity of Antioxidant Enzymes and Elevating Accumulation of Compatible Solutes Play Crucial Roles in Conferring Salt Tolerance to Sunflowers

Oxidative damage is a characteristic of plants in response to salt stress. Although low ROS can play roles as signal molecule, excessive accumulation of ROS induces lipid peroxidation, increases membrane leakage and reduces membrane fluidity, which is also thought to be the main cause of damage to membrane-localized proteins associated with ion channels, receptors and enzyme structures (Hao et al., 2021). ROS levels are controlled by antioxidants and ROS-scavenging enzymes. The accumulation of proline and other compatible solutes allows plants to reduce the osmotic potential and maintain cell swelling to facilitate normal physiological activities under salt stress. The accumulated solutes act as osmoprotectants to protect cells and maintain membrane integrity (Elsawy et al., 2018; Chahine et al., 2021). In this study, the salt-tolerant germplasms 182265 and 182283 had low levels of ROS (H_2O_2 and O_2^-) (**Figure 3F-I**), high activities of ROS-scavenging enzymes (APX, POD, CAT, and GR) (**Figure 4**), high total antioxidant capacity (T-AOC) (**Figure 4L**), and less cell damage (MDA and EL) (**Figure 3D-E** and **J-K**) under salt stress. Our results are consistent with research reports conducted in rice (Zhang et al., 2016), oilseed rape (Wan et al., 2022), barley (Nasrallah et al., 2022), cotton (Guo et al., 2019), wheat (Quan et al., 2021) and sugar beet (Geng et al., 2019). In salt-tolarant sunflower genotypes, compatible solute contents in leaves and roots also increased more significantly under salt stress with elevated more expression of corresponding genes, such as *HaP5CS* gene than salt-sensitive ones (**Figure 5**). Furthermore, the activities of ROS-scavenging enzymes showed positive relationships with the expression of the corresponding genes, there were higher enzyme activities and gene expression in salt-tolerant genotypes 182265 and 182283 than in salt- sensitive genotypes 182093, 186096 (**Figure 4C-D** and **Figure 7C-D**). These results suggest

 doi:10.20944/preprints202410.1786.v1

that salt-tolerant sunflowers have higher antioxidant enzyme activities and more osmoregulatory substances that maintain salt tolerance.

The Accumulation of Lower Na^+ and Higher K^+ Maintain a Good Growth for Salt Tolerant Sunflower

Salt stress is usually associated with excess NaCl-induced ionic toxicity. Thus, having a greater Na^+ efflux and barrier capacity is essential for salt tolerance in plants (Shahid et al., 2020). In salt-tolerant resources of chickpea, Na^+ accumulated preferentially in epidermal cells, and the rate of Na^+ translocation from roots to the above-ground parts was low; therefore, the chloroplasts remained highly photosynthetically active under salt stress (Kotula et al., 2019). This study also showed the importance of Na^+ homeostasis in salt-tolerant sunflowers: a key difference was that salt-tolerant sunflower genotypes had lower Na^+ in the roots and leaves (**Figure 6**). When Na^+ levels are high in the body, NHXs regulated vesicular membrane transport proteins partition compartmentalised Na^+ and SOS pathway-regulated cytosolic transport proteins excrete Na^+ (**Machnicka** et al., 2014). We examined the level of expression of the Na^+/H^+ transporter genes, i.e., *HaSOS1*, *HaSOS2*, and *HaSOS3*, as well as *HaNHXs* in the roots and leaves of two salt-tolerant differential sunflower genotypes under salt stress for 24 h. The results showed that the expression levels of all genes were higher in the salt-tolerant differential genotypes than in the salt-sensitive genotypes (**Figure 7**). We assumed that salt-tolerant germplasms have a stronger ability to exclude Na^+ through the plasma membrane Na^+/H^+ antitransporter. Reports indicated that plants often suffered from K^+ deficiency in high-salt environments due to the competitive inhibition by Na^+ (Zhao et al., 2020). Our findings aligned with this. Salt-tolerant resources have a higher K^+ content than sensitive resources.

Conclusion

Sunflower salt tolerance was comprehensively evaluated at the physiological level using salt-tolerant and salt-sensitive germplasms. Salt-tolerant sunflower genotypes have a relative healthy growth under salt stress, due to stronger photosynthesis, higher antioxidant enzyme activities, greater cellular osmotic regulation ability, and lower Na^+, higher K^+. This study provided valuable information on deeply exploring molecular mechanisms on salt tolerance and accelerating sunflower breeding process.

Supplementary Materials: The following supporting information can be downloaded at the website of this paper posted on Preprints.org. Please refer to the attachment.

Author Contributions: Y.Z., F.C., and L.X. conceived and designed the experiments; L.X., F.C., Q.H., Q.L., and X.H. performed the experiments; F.C., and L.X. analyzed the data and drafted the manuscript; and Y.Z. revised the manuscript. Z.L., and L.X. provided experimental materials and some suggestions. All authors have read and approved the contents of this manuscript.

Funding: This study was financially supported by Major Special Project 4 of Xinjiang Uygur Autonomous Region (No.2022A03004-4), the Natural Science Foundation of Xinjiang Uygur Autonomous Region (No. 2020D01C020), and the Research and Innovation Program for Excellent Doctoral Students at Xinjiang University (XJU2022BS050).

Conflicts of Interest: The authors declare no conflict of interest.

Acknowledgments: We extend our heartfelt thanks to the Institute of Economic Crops, Xinjiang Academy of Agricultural Sciences. We are also grateful to Dr. Chengxia Lai and Hong Sha for granting us access to essential experimental equipment. Furthermore, we deeply appreciate the meticulous and constructive feedback from the four reviewers, which significantly contributed to the improvement of this article.

Statements: Experimental and field research on plants was carried out in strict compliance with relevant institutional, national, and international guidelines and legislation, including the collection and cultivation of

plant material; all methods in regard to plants were carried out in accordance with relevant guidelines in the method section.

Data Availability Statement: All data generated or analyzed during this study are included in this published article [and its supplementary information files].

References

1. Abd-Elbar, O. H., Farag, R. E., Eisa, S. S., and Habib, S. A. (2012). Morpho-anatomical changes in salt stressed kallar grass (*Leptochloa fusca* L. Kunth). *Res J Agric Biol Sci*. 2, 158-166. doi: 10.1111/j.1469-8137.2006.01723.x
2. Agarwal, S. V., and Pandey, V. (2004). Antioxidant enzyme responses to NaCl stress in *Cassia angustifoli*. *Biol Plant*. 48, 555-560. doi: 10.1023/b:biop.0000047152.07878.e7
3. Amin, V. M., and Olson, N. F. (1967). Spectrophotometric determination of hydrogen peroxide in milk. *J Dairy Sci*. 50(4), 461-464. https://doi.org/10.3168/jds.S0022-0302(67)87447-2
4. Arnon, D. I. (1949). Copper enzymes in isolated chloroplasts. Polyphenoloxidase in *Beta vulgaris*. *Plant Physiol*. 24, 1-15. doi: 10.1104/pp.24.1.1
5. Bakhoum, G. S., Sadak, M. S., and Badr, E. A. E. M. (2020). Mitigation of adverse effects of salinity stress on sunflower plant (*Helianthus annuus* L.) by exogenous application of chitosan. *Bull Nat Research Centre*. 44(1), 1-11. https://doi.org/10.1186/s42269-020-00343-7
6. Benzie, I. F., Strain, J. J. (1996). The ferric reducing ability of plasma (FRAP) as a measure of "antioxidant power": the FRAP assay. *Anal Biochem*. 15, 239(1), 70-76. doi: 10.1006/abio.1996.0292. PMID: 8660627
7. Bodelón, O. G., Blanch, M., Sanchez-Ballesta, M. T., Escribano, M. I., and Merodio, C. (2010). The effects of high CO_2 levels on anthocyanin composition, antioxidant activity and soluble sugar content of strawberries stored at low non-freezing temperature. *Food Chem*. 122(3), 673-678. doi: 10.1016/j.foodchem.2010.03.029
8. Buysse, J. A. N., and Merckx, R. (1993). An improved colorimetric method to quantify sugar content of plant tissue. *Environ Exp Bot*. 44(10), 1627-1629. doi: 10.1093/jxb/44.10.1627
9. Cai, B. B., Li, Q., Liu, F. J., Bi, H. G., and Ai, X. Z. (2017). Decreasing fructose-1,6 -bisphosphate aldolase activity reduces plant growth and tolerance to chilling stress in tomato seedlings. *Physiol Plant*. 163(2), 247-258. doi: 10.1111/ppl.12682
10. Caverzan, A., Gisele, P., Barcellos, R. S., Werner, R. C., Fernanda, L., and Márcia, M. P. (2012). Plant responses to stresses: role of ascorbate peroxidase in the antioxidant protection. *Genet Mol Biol*. 35(4), 1011-1019. doi: 10.1590/s1415-47572012000600016
11. Chahine, S., Giannini, V., Roggero, P. P., and Melito, S. (2020). First insight of exogenous addition of proline and glycinebetaine to mitigate fluorine toxicity effects on common bean seedlings. *Italian J Agron*. 16(2), 1754. doi: 10.4081/ija.2020.1754
12. Demiral, T., and Türkan, I. (2005). Comparative lipid peroxidation, antioxidant defense systems and proline content in roots of two rice cultivars differing in salt tolerance. *Environ Exp Bot*. 53, 247-257. doi: 10.1016/j.envexpbot.2004.03.017
13. de Oliveira, V. P., Lima, M. D. R., da Silva, B. R. S., Batista, B. L., and da Silva Lobato, A. K. (2019). Brassinosteroids confer tolerance to salt stress in *Eucalyptus urophylla* plants enhancing homeostasis, antioxidant metabolism and leaf anatomy. *J Plant Growth Regul*. 38, 557-573. doi: 10.1007/s00344-018-9870-3
14. Doerge, D. R., Divi, R. L., and Churchwell, M. I. (1997). Identification of the colored guaiacol oxidation product produced by peroxidases. *Anal Biochem*. 250(1), 10-17. doi: 10.1006/abio.1997.2191
15. Elsawy, H. I. A., Mekawy, A. M. M., Elhity, M. A., Abdel-dayem, S. M., Abdelaziz, M. N., et al. (2018). Differential responses of two Egyptian barley (*Hordeum vulgare* L.) cultivars to salt stress. *Plant Physiol Biochem*. 127, 425-435. https://doi.org/10.1016/j.plaphy.2018.04.012
16. Estrada, Y., Fernández-Ojeda, A., Morales, B., Egea-Fernández, J. M., Flores, F. B., et al. (2021). Unraveling the strategies used by the underexploited amaranth species to confront salt stress: Similarities and differences with quinoa species. *Front Plant Sci*. 12, 604481. https://doi.org/10.3389/fpls.2021.604481
17. Geng, G., Lv, C. H., Stevanato, P., Li, R. R., Liu, H., Yu, L. H., et al. (2019). Transcriptome analysis of salt-sensitive and tolerant genotypes reveals salt-tolerance metabolic pathways in sugar beet. *Int J Mol Sci*. *20*(23), 5910. doi: 10.3390/ijms20235910
18. Giannopolitis, C. N., and Ries, S. K. (1977). Superoxide dismutases, occurrence in higher plants. *Plant Physiol*. 59, 309-314. doi: 10.1104/pp.59.2.309
19. Guo, H. J., Hu, Z. Q., Zhang, H. M., Min, W., and Hou, Z. N. (2019). Comparative effects of salt and alkali stress on antioxidant system in Cotton (*Gossypium Hirsutum* L.) Leaves. *Open Chem*. 17(1), 1352-1360. doi: 10.1515/chem-2019-0147

20. Hao, S. H., Wang, Y. R., Yan, Y. X., Liu, Y. H., Wang, J. Y., and Chen, S. (2021). A review on plant responses to salt stress and their mechanisms of salt resistance. *Horticulturae*. 7(6), 132. https://doi.org/10.3390/horticulturae7060132
21. Hou, P. C., Wang, F. F., Luo, B., Li, A. X., Wang, C., Shabala, L., et al. (2021). Antioxidant enzymatic activity and osmotic adjustment as components of the drought tolerance mechanism in *Carex duriuscula*. *Plants*. 10(3), 1-20. doi: 10.3390/plants10030436
22. Jiang, D., Lu, B., Liu, L. T., Duan, W. J., Meng, Y. J., Li, J., et al. (2021). Exogenous melatonin improves the salt tolerance of cotton by removing active oxygen and protecting photosynthetic organs. *BMC Plant Biol*. 21, 331. doi: 10.1186/s12870-021-03082-7
23. Johansson, L. H., and Borg, L. A. H. (1988). A spectrophotometric method for determination of catalase activity in small tissue samples. *Anal Biochem*. 174(1), 331-336. https://doi.org/10.1016/0003-2697(88)90554-4
24. Kiani-Pouya, A., Roessner, U., Jayasinghe, N. S., Lutz, A., Rupasinghe, T., Bazihizina, N., et al. (2017). Epidermal bladder cells confer salinity stress tolerance in the halophyte quinoa and Atriplex species. *Plant Cell Environ*. 40(9), 1900 - 1915. doi: 10.1111/pce.12995.
25. Kotula, L., Clode, P. L., De La Cruz Jimenez, J., and Colmer, T. D. (2019). Salinity tolerance in chickpea is associated with the ability to 'exclude' Na from leaf mesophyll cells. *J Exp Bot*. 70(18), 4991-5002. doi: 10.1093/jxb/erz241
26. Li, J. P., Liu, J., Zhu, T. T., Zhao, C., Li, L. Y., and Chen, M. (2019). The role of melatonin in salt stress responses. *Int J Mol Sci*. 20(7), 1735. https://doi.org/10.3390/ijms20071735
27. Li, J. P., Yuan, F., Liu, Y. L., Zhang, M. J., Liu, Y., Zhao, Y., et al. (2020). Exogenous melatonin enhances salt secretion from salt glands by upregulating the expression of ion transporter and vesicle transport genes in *Limonium bicolo. BMC Plant Biol*, 20, 493. https://doi.org/10.1186/s12870-020-02703-x
28. Li, W. J., Meng, R., Liu, Y., Chen, S. M., Jiang J. F., Wang, L. K., et al. (2022). Heterografted *chrysanthemums* enhance salt stress tolerance by integrating reactive oxygen species, soluble sugar, and proline. *Hortic Res*. 9, 73. doi: 10.1093/hr/uhac073
29. Li, W. H., Zhang, H. Z., Zeng, Y. L., Xiang, L. J., Lei, Z. H., Huang, Q. X., et al. (2020). A salt tolerance evaluation method for sunflower (*Helianthus annuus* L.) at the seed germination stage. *Sci Rep*. 10(1), 10626. doi: 10.1038/s41598-020-67210-3
30. Liu, X. H., Cai, S. G., Wang, G., Wang, F. F., Dong, F. B., Mak, M., et al. (2017). Halophytic NHXs confer salt tolerance by altering cytosolic and vacuolar K^+ and Na^+ in *Arabidopsis* root cell. *Plant Growth Regul*. 82(2), 333-351. doi: 10.1007/s10725-017-0262-7
31. Liu, Y., Su, M. X., and Han, Z. J. (2022). Effects of NaCl stress on the growth, physiological characteristics and anatomical structures of *Populus talassica×Populus euphratica* seedlings. *Plants (Basel, Switzerland)*. 22 (11), 3025-3051. https://doi.org/10.3390/plants11223025
32. Long, L., Zhao, J. R., Guo, D. D., Ma, X. N., Xu, F. C., Yang, W. W., et al. (2020). Identification of NHXs in gossypium species and the positive role of *GhNHX1* in salt tolerance. *BMC Plant Biol*. 20(1), 147. doi: 10.1186/s12870-020-02345-z
33. **Machnicka, B., Czogalla, A., Hryniewicz-Jankowska, A., Bogusławska, D. M., Grochowalska, R., Heger, E.,** et al**. (2014). Spectrins: A structural platform for stabilization and activation of membrane channels, receptors and transporters. *BBA-Biomembranes*. 1838(2), 620-634.** doi: 10.1016/j.bbamem.2013.05.002
34. Nadarajah, K. K. (2020). ROS homeostasis in abiotic stress tolerance in plants. *Int J Mol Sci*. 21(15), 5208. doi: 10.3390/ijms21155208
35. Nasrallah, A. K., Atia, M. A. M., Abd El-Maksoud, R. M., Kord, M. A., and Fouad, A. S. (2022). Salt priming as a smart approach to mitigate salt stress in faba bean (*Vicia faba* L.). *Plants (Basel)*. 11(12), 1610. doi: 10.3390/plants11121610
36. Nassar, R. M. A., Kamel, H. A., Ghoniem, A. E., Alarcón, J. J., Sekara, A., Ulrichs, C., et al. (2020). Physiological and anatomical mechanisms in wheat to cope with salt stress induced by seawater. *Plants*. 9(2), 237. doi: 10.3390/plants9020237
37. **Periasamy, K. (1967). A technique of staining sections of paraffin-embedded plant materials without employing a graded ethanol series. *J R Microsc Soc*. 87(1), 109-112.** doi: 10.1111/j.1365-2818.1967.tb04496.x
38. Quan, X. Y., Liang, X. L., Li, H. M., Xie, C. J., He, W. X., and Qin, Y. X. (2021). Identification and characterization of wheat germplasm for salt tolerance. *Plants Basel*. 10(2), 268. doi: 10.3390/plants10020268
39. Reuveni R. (1992). Peroxidase activity as a biochemical marker for resistance of muskmelon (*Cucumis melo*) to *Pseudoperonospora cubensis*. *Phytopathology*. 82(7), 749-753. doi: 10.1094/phyto-82-749
40. Sanwal, S. K., Kumar, P., Kesh, H., Gupta, V. K., Kumar, A., Kumar, A., et al. (2022). Salinity stress tolerance in potato cultivars: evidence from physiological and biochemical traits. *Plants (Basel)*. 11(14), 1842. https://doi.org/10.3390/plants11141842
41. Satterfield, C. N., and Bonnell, A. H. (1955). Interferences in titanium sulfate method for hydrogen peroxide. *Anal Chem*. 27(7), 1174-1175. doi: 10.1021/ac60103a042
42. Scopes, R., (1987). Protein purification: principles and practice, 3rd Edn. New York, NY: Springer-Verlag, Inc. doi: 10.1007/978-1-4757-1957-4

43. Sedmak, J. J., and Grossberg, S. E. (1977). A rapid, sensitive and versatile assay for protein using Coomassie brilliant blue G 250. *Anal Biochem*. 79, 544-552. doi: 10.1016/0003-2697(77)90428-6
44. Shabala, S. N., and Lew, R. R. (2014). Turgor regulation in osmotically stressed *Arabidopsis* epidermal root cells. Direct support for the role of cell turgor measurements. *Plant Physiol*. 129, 290-299. doi: 10.1104/pp.020005
45. Shahid, M. A., Sarkhosh, A., Khan, N., Balal, R. M., Ali, S., Rossi, L., et al. (2020). Insights into the physiological and biochemical impacts of salt stress on plant growth and development. *Agronomy*. 10(7), 938. doi: 10.3390/agronomy10070938
46. Shigeoka, S., Nakano, Y., and Kitaoka, S. (1980). Metabolism of hydrogen peroxide in *Euglena gracilis* Z by L-ascorbic acid peroxidase. *Biochem J*. 186(1), 377-380. doi: 10.1042/bj1860377
47. Shokoofeh, H., Milan, S., Marian, B., and Vachova, P. (2021). Effect of sodium nitroprusside on physiological and anatomical features of salt-stressed *Raphanus sativus*. *Plant Physiol Bioch*. 169, 160-170. doi: 10.1016/j.plaphy.2021.11.013
48. Shumilina, J., Kusnetsova, A., Tsarev, A., Van Rensburg, H. C. J., Medvedev, S., Demidchik, V., et al. (2019). Glycation of plant proteins: regulatory roles and interplay with sugar signalling? *Int J Mol Sci*. 20(9), 2366. doi: 10.3390/ijms20092366
49. Spitz, D. R., and Oberley, L. W. (1989). An assay for superoxide dismutase activity in mammalian tissue homogenates. *Anal Biochem*, 179(1), 8-18. doi: 10.1016/0003-2697(89)90192-9
50. Taher, M., Beyaz, R., Javani, M., Gürsoy, M., and Yildiz, M. (2018). Morphological and biochemical changes in response to salinity in sunflower (*Helianthus annus* L.) cultivars. *Ital J of Agron*. 13(2), 141-147. https://doi.org/10.4081/ija.2018.1096
51. Wan, H., Qian, J., Zhang, H., Lu, H., Li, O., Li, R., et al (2022). Combined transcriptomics and metabolomics analysis reveals the molecular mechanism of salt tolerance of Huayouza 62, an eite cultivar in rapeseed (*Brassica napus* L.). *Int J Mol Sci*. 23(3), 1279. doi: 10.3390/ijms23031279
52. Yuan, Y. H., Wu, C. Y., Liu, L., Ma, Q., Yang, Q. H., and Feng, B. L. (2021). Unravelling the distinctive growth mechanism of proso millet (*Panicum miliaceum* L.) under salt stress: From root-to-leaf adaptations to molecular response. *GCB Bioenergy*, 14(2), 192-214. doi: 10.1111/gcbb.12910
53. Zeeshan, M., Lu, M., Sehar, S., Holford, P., and Wu, F. (2020). Comparison of biochemical, anatomical, morphological, and physiological responses to salinity stress in wheat and barley genotypes deferring in salinity tolerance. *Agronomy*. *10(1)*, 127. doi: 10.3390/agronomy10010127
54. Zhang, H. M., Zhu, J. H., Gong, Z. Z., and Zhu, J. K. (2022). Abiotic stress responses in plants. *Nat Rev Genet*. 23(2), 104-119. doi: 10.1038/s41576-021-00413-0
55. Zhang, J. Y., Luo, W., Zhao, Y., Xu, Y. Y., Song, S. H., and Chong, K. (2016). Comparative metabolomic analysis reveals a reactive oxygen species-dominated dynamic model underlying chilling environment adaptation and tolerance in rice. *New Phytol*. 211(4), 1295-1310. doi: 10.1111/nph.14011
56. Zhang, N., Zhao, B., Zhang, H. J., Weeda, S., Yang, C., Yang, Z. C., et al. (2012). Melatonin promotes water stress tolerance, lateral root formation, and seed germination in cucumber (*Cucumis sativus* L.). *J Pineal Res*. 54(1), 15-23. doi: 10.1111/j.1600–079X.2012.01015.x
57. Zhao, C. Z., Zhang, H., Song, C. P., Zhu J. K., and Shabala, S. (2020). Mechanisms of plant responses and adaptation to soil salinity. *The Innovation*. 1(1), e100017. doi: 10.1016/j.xinn.2020.100017